Can sea surface height be used to estimate oceanic transport variability?

V. O. Ivchenko,[1,2] D. Sidorenko,[1] S. Danilov,[1] M. Losch,[1] and J. Schröter[1]

Received 8 March 2011; revised 28 April 2011; accepted 29 April 2011; published 2 June 2011.

[1] The relation between the sea surface height and the meridional transport across a zonal section at 26.5°N in the North Atlantic is studied by using an eddy resolving ocean state estimate simulated with the Massachusetts Institute of Technology general circulation model. It is shown that the correlation between the zonal sea surface height difference and transport can be substantially increased if the steric height contribution from the seasonal thermocline is removed. The latter explains a substantial part of sea surface height variability, but its effect on transport is weak. It is also found that the zonal steric height difference correlates well with the transport after the contribution of the seasonal thermocline has been removed. There is a similar agreement (with correlation coefficient of 0.63 for the full signal and 0.89 for the mean seasonal cycle) between the meridional transport and steric height based on observations from the Rapid Climate Change (RAPID) project. **Citation:** Ivchenko, V. O., D. Sidorenko, S. Danilov, M. Losch, and J. Schröter (2011), Can sea surface height be used to estimate oceanic transport variability?, *Geophys. Res. Lett.*, *38*, L11601, doi:10.1029/2011GL047387.

1. Introduction

[2] The Atlantic meridional overturning circulation (AMOC) comprises an upper ocean northward flow in a warm water layer of about 1000 m and a compensating southward return flow in the deeper ocean. The northward flow provides approximately one-quarter of the global meridional heat transport [see, e.g., *Hall and Bryden*, 1982; *Kanzow et al.*, 2007, 2009, 2010]. This heat transport represents an important factor for the European climate. The variability of the AMOC has therefore the potential of monitoring a changing European climate. For this reason estimating this variability on different time scales and understanding the underlying mechanisms become important.

[3] One usually distinguishes between fast (from days to a few weeks), seasonal and interannual variability of the AMOC. Within this definition, the fast constituent is the most energetic one [*Cunningham et al.*, 2007; *Kanzow et al.*, 2007] with amplitudes reaching 10 Sv or even more. But even after low-pass filtering the observed combined seasonal and interannual variability retains a very strong signal of 5–7 Sv.

[4] Direct measurements of meridional transport across a zonal section, for example 26.5°N in the Northern Atlantic, that would allow assessing the transport variability and studying its mechanisms, are expensive. As high quality satellite altimetry data become available, it is interesting to ask whether there is a link between the sea surface height (η) along and the meridional transport across a zonal section. Several authors suggested to use η field as an indicator of transport variability [*Fukumori et al.*, 1998; *Tierney et al.*, 2000; *Vinogradova et al.*, 2007; *Hirschi et al.*, 2009]. *Hirschi et al.* [2009] demonstrated that η can be used for this purpose in the Northern Atlantic at 26°N if the western and eastern parts of the section are considered separately. They found significant correlations of 0.3–0.9 between the zonal η differences and the meridional transport in the upper 1100 m. Much weaker correlations were found for the basin wide transport. The latter circumstance was attributed to the relative importance of the reversal currents close to the western coast by *Kanzow et al.* [2009]. The results of their study suggest that the basin wide difference in η cannot provide a reliable estimate of the meridional transport variability.

[5] In this study we return to the question whether the variability in the η fields can be used as a proxy for the meridional transport variability on seasonal and interannual time scales. We demonstrate that η can serve this purpose, but only in the combination with steric height (η_{st}). Following *Hirschi et al.* [2009] we concentrate on the zonal section at 26.5°N in the North Atlantic. It consists of the mid-ocean transatlantic section between the Bahamas and Africa and the section through the Florida Straits (about 80 km). The Gulf Stream transport through the Straits can be derived from cable voltage measurements across the Straits [*Cunningham et al.*, 2007]. For this reason we focus on the midocean transatlantic section. The analysis is based on a numerical simulation by the Massachusetts Institute of Technology general circulation model (MITgcm) (MITgcm Group, MITgcm User Manual, MIT/EAPS, online documentation, Cambridge, Massachusetts, 2010, available at http://mitgcm.org/public/r2_manual/latest/online_documents/manual.html).

[6] We relate the simulation-based investigation to reality by showing that our analysis might be useful in interpreting indirect observations of the AMOC within the UK Natural Environment Research Council Rapid Climate Change (RAPID) project.

2. Model and Observational Data

[7] Monthly fields of temperature, salinity, velocity, and sea surface height from an ECCO2 global ocean model simulation for 1992 to 2007 with a mean horizontal resolution of 18 km are used; this particular simulation is labeled "cube78", it is available at http://ecco2.jpl.nasa.gov/data1/cube/cube78. The ocean model setup is very similar to those

[1]Alfred Wegener Institute for Polar and Marine Research, Bremerhaven, Germany.
[2]National Oceanography Centre, Southampton, UK.

Copyright 2011 by the American Geophysical Union.
0094-8276/11/2011GL047387

described by *Losch et al.* [2010] and *Menemenlis et al.* [2008].

[8] The model data is analysed along the mid ocean part (from 76.5°W to 16°W) of the 26.5°N section. Due to the cubed-sphere grid configuration of the ocean model the section is not aligned with a latitude circle but follows an arc passing through 26.5°N at both ends and 24°N at about 45°W. Following other studies we associate the AMOC variability with that of the transport in the upper 1000 m.

[9] The use of simulated data facilitates the analysis greatly. However, we note that the climatology formed from the model data has the same characteristics along 26.5°N as climatology derived from observations [*Conkright et al.*, 2002]. We refrain from showing a direct comparison of model data and observations, because they are so similar.

[10] The RAPID array data provides unique monitoring of the basin scale circulation along 26.5°N in Atlantic from April 2004 [*Bryden et al.*, 2009; *Cunningham et al.*, 2007; *Hirschi et al.*, 2009; *Kanzow et al.*, 2007, 2009, 2010]. A detailed map with the locations of moorings is given by *Kanzow et al.* [2009, Figure 2]. The data comprises not only profiles of temperature, salinity, and pressure, but also co-located bottom pressure time series. This allows to evaluate dynamic pressure from surface to bottom and therefore the upper mid-ocean meridional transport time series. The latter has been analysed for the upper 1100 m [see, e.g., *Cunningham et al.*, 2007]. In the current study the vertical profiles of temperature in the western and eastern points of the section are used for the calculation of steric height.

3. Steric Height and Meridional Transport

[11] Outside the boundary layers the flow through the section is approximately in geostrophic balance, so that the AMOC streamfunction Ψ can be split into the Ekman Ψ_{Ek} and the geostrophic Ψ_{geo} parts. The Ekman part can easily be calculated from the zonal wind stress τ_x, and its seasonal cycle ranges from −1 to +2 Sv [*Atkinson et al.*, 2010].

[12] We focus on the geostrophic part of the meridional transport, which is the integral of the meridional component of geostrophic velocity over the section. The geostrophic velocity is proportional to the zonal pressure gradient so that the transport is determined by the vertically integrated pressure difference between the end-points of the section. Since the pressure difference at depth z depends on the differences in η and in η_{st} computed relative to z, we expect that variations of Ψ_{geo} correlate with $\Delta\eta$, but we also expect that the steric height signal from the seasonal thermocline reduces this correlation. Here Δ is the operator of difference between the western and eastern ends of the section.

[13] We will show below that a substantial part of the variability of the $\Delta\eta$ has indeed a small projection on the transport variability. This part is identified with the variability of the steric height differences that stem from incoming vertical heat fluxes through the surface.

3.1. Variability of Steric Height

[14] In what follows we will deal with anomalies of η and η_{st}. The η anomaly η' can be split in two components [*Gill and Niiler*, 1973],

$$\eta' = \eta'_{st} + \frac{p'_b}{g\rho_0}, \tag{1}$$

where η'_{st} and p'_b are the anomalies in steric height and bottom pressure, respectively, g is the gravitational acceleration and ρ_0 the constant reference density.

[15] The changes in steric height are caused by the changes in density due to expansion or contraction

$$\eta'_{st} = \frac{1}{g\rho_0}\int_{p_b}^{p_s} \delta\, dp, \tag{2}$$

where δ is the specific volume anomaly computed from the equation of state and p_s is the surface pressure. The difference between η' and η'_{st} is the bottom pressure signal. It directly reflects mass redistributions, in particular changes in barotropic motion and net freshwater flux at the surface (precipitation-evaporation).

[16] We somewhat arbitrarily divide the ocean at the zonal section of 26.5°N in 3 layers: the seasonal thermocline (between the surface and 200 m), main thermocline (above 1000 m), and deep ocean (below 1000 m; a larger depth of 1100 m is used by *Hirschi et al.* [2009]). We anticipate that steric height variability in the two upper layers will map onto transport variability in different ways. The steric height is also split into contributions from these layers (i.e., from the seasonal thermocline, main thermocline and the abyss).

[17] *Gill and Niiler* [1973] demonstrated that the variability in heat and salt content within the seasonal thermocline is mainly determined by the surface buoyancy fluxes; lateral advection is less important. The incoming heat flux forces locally a strong seasonal cycle onto temperature leading to high variability of steric expansion in the seasonal thermocline, and as consequence, of η. In the numerical model data, the variability of the steric height anomalies of the seasonal thermocline (taken to be the top 200 m) η'^{200}_{st} explains approximately 43% of the variability of the steric height anomalies within the entire main thermocline (down of 1000 m) η'^{1000}_{st} and 40% of the η' variability.

[18] The level of 95% significance is computed with the two-tailed test and degrees of freedom corrected for lag-1 autocorrelation. The effective sample size for the monthly time series was above 110 for all quantity pairs implying that all correlations above 0.19 are significant. In the view of this, we omit providing the levels of significance in the text below.

[19] The contribution by density changes in the intermediate layer (200–1000 m) to the steric height anomalies is similarly large or even larger than that of the upper layer. However, surface buoyancy fluxes are unlikely to reach this layer on the time scale of a few years that are considered here. Contributions from the intermediate layer are mainly attributed to dynamical processes that involve vertical displacements of isopycnals.

[20] The contribution of the deep layer (beneath the main thermocline) to the interannual steric height anomaly is much smaller than the contributions from the seasonal and main thermocline [*Ivchenko et al.*, 2008]. For this reason we can neglect this layer completely in the context of interannual variability (the variability of η'^{1000}_{st} explains 93% of η' variability in model data).

[21] The contribution of the seasonal thermocline to the steric height variability is large, but there is very little transport associated with it because thermal expansion and contraction does not change the mass in the layer, and because the variability is confined to a thin layer (less than

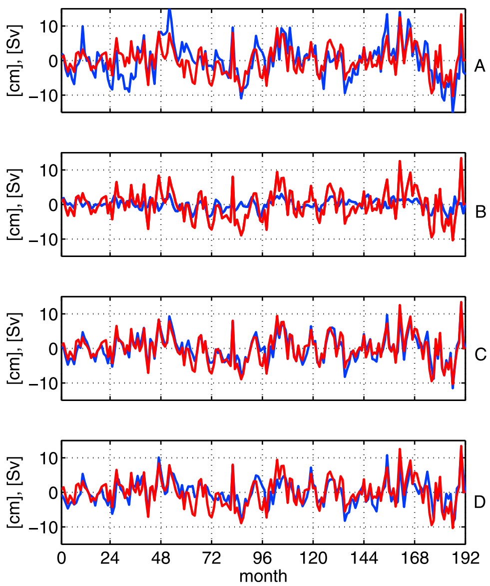

Figure 1. Temporal variability of the geostrophic meridional transport in the upper 1000 m (red line) and dynamical height differences (blue lines) (a) $\Delta\eta'$, (b) $\Delta(\eta' - \eta_{st}'^{1000})$, (c) $\Delta(\eta' - \eta_{st}'^{200})$ and (d) $\Delta(\eta_{st}'^{1000} - \eta_{st}'^{200})$ in MITgcm output data. Units are Sverdrups for transport and centimeters for dynamical heights.

200 m). Hence the associated pressure gradient integrated to the bottom of the seasonal thermocline does not change substantially over the season. The maximum steric height difference between the eastern and western points due to the thermal expansion of the seasonal thermocline as computed from *Conkright et al.* [2002] climatology is about 7 cm (March minus September). The corresponding transport anomaly, assuming zero pressure change at 200 m, is about 0.5 Sv. It is still small compared to the commonly observed variability of AMOC of a few Sverdrup.

3.2. Variability of the Meridional Transport and Its Link to Sea Surface Height and Steric Height

[22] After explaining the contributions of the different layers to the sea surface height variability, we now examine relationship between the sea surface height and the geostrophic transport variability at 26.5°N. We use again the simulated data because the RAPID times series for the upper 200 m is not complete. The 26.5°N-section does not extend into the western frictional boundary layer, so that the modeled geostrophic transport can be backed out approximately as the difference between the total transport and the Ekman transport. There is a correlation of 0.70 between the monthly mean values of geostrophic transport and $\Delta(\eta')$ over the 16 years of simulation (see Figure 1a). The correlation is even larger (0.78, see Figure 2 and Table 1) for the mean seasonal cycle.

[23] *Kanzow et al.* [2009] observed a similar correlation of 0.71 when they choose their western end point at 76.5°W. They show that if the end point is moved further west the correlation reduces to 0.44 at 76.75°W and 0.12 at 76.82°W (see Figure 4). *Kanzow et al.* [2009] demonstrated that the reduced correlation is associated with current components with increasingly stronger vertical reversal within the vicinity of the western coast. In the present study we can also observe reduction in correlations to 0.62 at 76.75°W and 0.5 at 76.92°W. These values, however, are still high (see Figure 4) compared to *Kanzow et al.* [2009].

[24] Hence there is a part of the geostrophic transport (i.e., the integrated pressure gradient) variability that is not explained by the difference in η'. We determine which part of the water column contributes to the full signal by removing the steric height anomaly relative to the upper 1000 m ($\eta_{st}'^{1000}$) and relative to the upper 200 m ($\eta_{st}'^{200}$) from η' (Figures 1b and 1c).

[25] The correlation between $\Delta(\eta' - \eta_{st}'^{1000})$ and the geostrophic transport (0.56) is much lower than between $\Delta\eta'$ and transport for the full time series and insignificant for the averaged seasonal cycle (0.04). For $\Delta(\eta' - \eta_{st}'^{200})$, the time series agrees much better with the geostrophic transport than for $\Delta(\eta' - \eta_{st}'^{1000})$ and also $\Delta(\eta')$. The correlation is 0.90 for both the full time series and the averaged annual cycle.

[26] Thus, $\Delta(\eta' - \eta_{st}'^{1000})$ is only weakly related to transport anomalies. In contrast, the pressure difference just below the seasonal thermocline, $\Delta(\eta' - \eta_{st}'^{200})$, correlates with the geostrophic transport variability because by subtracting the signal of $\eta_{st}'^{200}$ we remove a large part of variability that is associated only with small changes in the transport. The analysis was repeated for the western end location of 76.92°W. This grid point is at the coast (the Bahamas) in the model, so all transport variability is accounted for. In this case, the correlation between $\Delta(\eta' - \eta_{st}'^{200})$ and transport variability is 0.84, so that we can conclude that our result remains valid.

[27] Small variation of the thickness of the seasonal thermocline (between 150m–200m–250m) and main thermocline (900m–1000m–1100m) did not strongly affect our results. Correlation between transport and differences in sea surface height with steric height from the seasonal thermocline removed is above 0.88 in all experiments and reached 0.92 when the seasonal thermocline was computed to 250 m.

[28] Unfortunately, it is not possible to derive the contribution of the upper 200 m to the steric height anomaly from the high temporal resolution data of RAPID because of data gaps. We tried to fill in these gaps by estimating the contribution from climatological steric height anomalies [*Conkright et al.*, 2002] and from model climatology (the mean seasonal cycle), but both methods failed to give

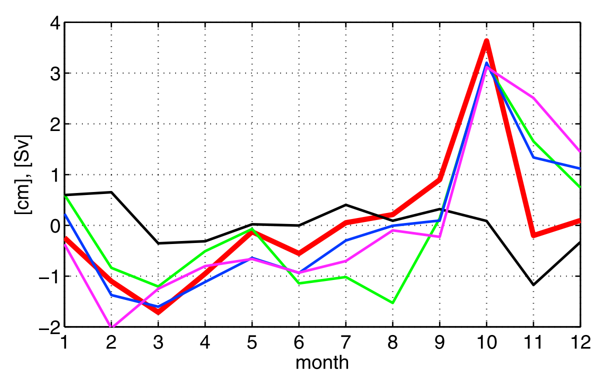

Figure 2. Seasonal variability of the geostrophic meridional transport in the upper 1000 m (red line) and of $\Delta(\eta')$ (green), $\Delta(\eta' - \eta_{st}'^{1000})$ (black), $\Delta(\eta' - \eta_{st}'^{200})$ (blue) and $\Delta(\eta_{st}'^{1000} - \eta_{st}'^{200})$ (magenta) in ECCO2/MITgcm output. Units are the same as in Figure 1.

Table 1. Correlations Between Meridional Geostrophic Transport and Dynamical Heights for the Total Period From 1992 to 2007 for ECCO2/MITgcm and From 2004 to 2009 for RAPID, and for the Seasonal Average

	η'	$\eta' - \eta'^{1000}_{st}$	$\eta' - \eta'^{200}_{st}$	$\eta'^{1000}_{st} - \eta'^{200}_{st}$	$\eta'^{1100}_{st} - \eta'^{200}_{st}$ (RAPID)
Total period	0.70	0.56	0.90	0.75	0.63
Seasonal average	0.78	0.04	0.90	0.77	0.89

acceptable correlations with the full time series of model geostrophic transport.

[29] RAPID hydrography data is generally available in the main thermocline layer below 200 m depth and the main contributions to transport variability is associated with that layer (i.e., 200 m to 1000 m or 1100 m). We therefore studied the link between the steric height variability due to the layer, $\Delta(\eta'^{1000}_{st} - \eta'^{200}_{st})$, and geostrophic transport variability. Although restricting oneself to $\Delta(\eta'^{1000}_{st} - \eta'^{200}_{st})$ removes a part of the barotropic signal visible in $\Delta(\eta' - \eta'^{200}_{st})$ it is still interesting to understand to what extent this influences the correlation.

[30] In this case we can use MITgcm simulation data and the RAPID data that is available for the period of time between April 2004 and April 2009. The correlation between the simulated $\Delta(\eta'^{1000}_{st} - \eta'^{200}_{st})$ and the corresponding variability of meridional transport is indeed high for both the whole period of 16 years (0.75) and for the averaged seasonal variability (0.77). It compares with the respective correlation for $\Delta\eta'$ but is lower than for $\Delta(\eta' - \eta'^{200}_{st})$ (see Figures 1 and 2 and Table 1).

[31] For the RAPID data, the variability of $\Delta(\eta'^{1000}_{st} - \eta'^{200}_{st})$ was compared with the mid ocean transports of *Cunningham et al.* [2007]. We found correlations of 0.63 between $\Delta(\eta'^{1000}_{st} - \eta'^{200}_{st})$ and the meridional transport for the whole RAPID period (see Figure 3 and Table 1), and 0.89 if only averaged seasonal variability was analysed. (Note that here, η'^{1000}_{st} is taken relative to 1100 m to be consistent with the estimates by *Cunningham et al.* [2007].

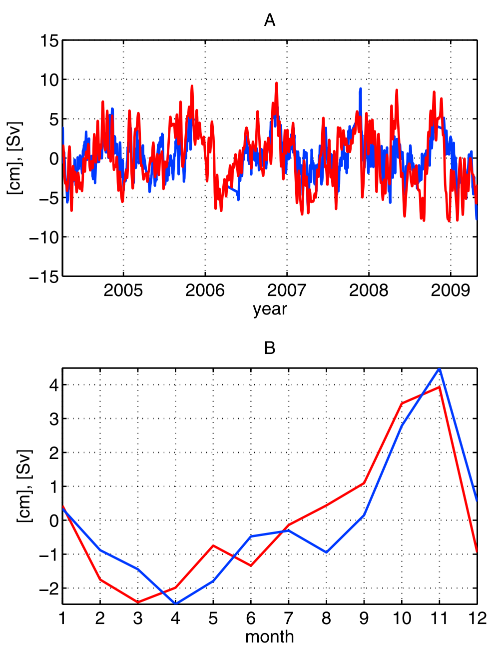

Figure 3. (a) Temporal variability and (b) seasonal variability of the meridional upper mid-ocean transport (upper 1100 m) (red line) and the dynamical height difference $\Delta(\eta'^{1000}_{st} - \eta'^{200}_{st})$ (blue line) based on the RAPID data of *Cunningham et al.* [2007]. Units are the same as in Figure 2.

4. Summary and Discussion

[32] Understanding the variability of the ocean circulation, in particular on interannual time scales, is an important objective of physical oceanography. We demonstrate that the correlation between the sea surface height and the AMOC at 26.5°N is improved if the steric height contribution from the seasonal thermocline is removed. Such modification removes a strong seasonal signal identified mostly with the steric expansion in the upper 200 m. Qualitatively its contribution to the transport behaves as the second mode of *Kanzow et al.* [2009], which reverses at about 150 m depth.

[33] Although the steric height variability due to the upper layer, as well as variability of associated subsurface velocities, are large, they do not lead to a mass redistribution, so that the contribution of this variability to the transport anomaly in the upper 1000 m stays small.

[34] The difference $\Delta(\eta' - \eta'^{200}_{st})$ is highly correlated with the meridional transport variability. This correlation decreases only slightly if we move the western end point of the computations further west from WB3. The decrease in correlation between the transport and $\Delta(\eta' - \eta'^{200}_{st})$ is much smaller than the reduction in correlation between the transport and $\Delta(\eta')$ shown in Figure 4. This suggests the feasibility of estimating the meridional transport variability by combining high quality satellite altimetry data with steric

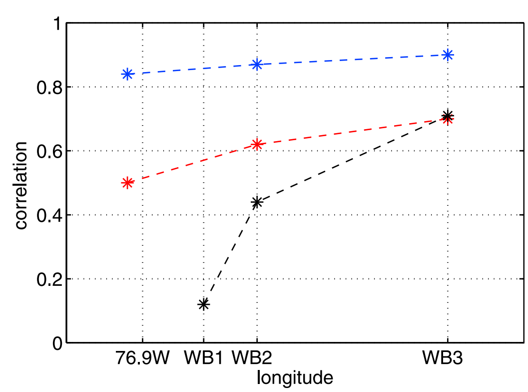

Figure 4. Correlations between $\Delta\eta'$ and transports in ECCO2 and by *Kanzow et al.* [2008] (red and black curves, respectively). The blue curve depicts the correlation between $\Delta(\eta' - \eta'^{200}_{st})$ and transport in ECCO2. The positions WB1, WB2 and WB3 correspond to those from *Kanzow et al.* [2008] and are 76.82°W, 76.75°W and 76.5°W, respectively.

height estimates from temperature profiles (e.g., by XBTs) at two points of a section. Gaps in the RAPID data in the upper 160 m for a substantial part of the measurement period prevent us from performing such an analysis today. Nevertheless we validated the feasibility of the proposed approach to observe AMOC fluctuations using a combination of altimetry and XBT measurements by adding uncertainties to the simulated model quantities. Normally distributed noise with standard deviations of 2 cm and 1 cm was added to η and $\eta_{st}'^{200}$, respectively. The averaged statistics (an ensemble of 100 realisations has been used) show that the correlations between transport and $\Delta(\eta' - \eta_{st}'^{200})$ drop from 0.90 to 0.78 and 0.83 for the total period and seasonal average respectively, and remain relatively high.

[35] Further, our analysis revealed a link between the baroclinic processes in the main thermocline below its seasonal part and the variability of meridional transport. Although the correlation between the variability of the steric height over the main thermocline depth below 200 m and the meridional transport is weaker than for the surface-corrected variability, our analysis shows substantial similarities between these quantities in both numerical simulations and RAPID data. Of course 16 years of the model run and 5 years of the RAPID observations are definitely not long enough to draw conclusions on the decadal variability. Additional studies are needed to learn about correlations on those scale.

[36] The improved correlation between the corrected sea surface height and transport anomalies might prove useful for the analysis of geostrophically balanced transport not only at 26.5°N but in other sections as well. This requires combining satellite altimetry data with the temperature and salinity measurements at the ends of a section, and calls for more specific studies of the accuracy of the method.

[37] **Acknowledgments.** We thank the RAPID team for providing high quality data, freely available from www.noc.soton.ac.uk/rapidmoc, and the ECCO2 team for making their data available. We thank J. Hirschi for valuable comments. The RAPID-WATCH MOC monitoring project is funded by the National Environment Research Council. We appreciate valuable comments from two anonymous reviewers.

[38] The Editor thanks the two anonymous reviewers for their assistance in evaluating this paper.

References

Atkinson, C. P., H. L. Bryden, J. J.-M. Hirschi, and T. Kanzow (2010), On the variability of Florida Straits and wind driven transports at 26°N in the Atlantic Ocean, *Ocean Sci. Discuss*, *6*, 837–859, doi:10.5194/os-6-837-2010.

Bryden, H. L., A. Mujahid, S. Cunningham, and T. Kanzow (2009), Adjustment of the basin-scale circulation at 26°N to variations in Gulf Stream, deep western boundary current and Ekman transports as observed by the Rapid array, *Ocean Sci.*, *5*, 421–433.

Conkright, M. E., et al. (2002), *World Ocean Atlas 2001*, NOAA, Silver Spring, Md.

Cunningham, S. A., et al. (2007), Temporal variability of the Atlantic meridional overturning circulation at 26.5°N, *Science*, *317*, 935–938, doi:10.1126/science.1141304.

Fukumori, I., R. Raghunath, and L.-L. Fu (1998), Nature of global large-scale sea level variability in relation to atmospheric forcing: A modeling study, *J. Geophys. Res.*, *103*, 5493–5512.

Gill, A. E., and P. P. Niiler (1973), The theory of the seasonal variability in the ocean, *Deep Sea Res. Oceanogr. Abstr.*, *20*, 141–177.

Hall, M. M., and H. L. Bryden (1982), Direct estimates and mechanisms of ocean heat transport, *Deep Sea Res., Part A*, *29*, 339–359.

Hirschi, J. J.-M., P. D. Killworth, J. R. Blundell, and D. Cromwell (2009), Sea surface height signals as indicators for oceanic meridional mass transport, *J. Phys. Oceanogr.*, *39*, 581–601, doi:10.1175/2008JPO3923.1

Ivchenko, V. O., S. Danilov, D. Sidorenko, J. Schröter, M. Wenzel, and D. L. Aleynik (2008), Steric height variability in the Northern Atlantic on seasonal and interannual scales, *J. Geophys. Res.*, *113*, C11007, doi:10.1029/2008JC004836.

Kanzow, T., S. A. Cunningham, D. Rayner, J. J.-M. Hirschi, W. E. Johns, M. O. Baringer, H. L. Bryden, L. M. Beal, C. S. Meinen, and J. Marotzke (2007), Observed flow compensation associated with the MOC at 26.5°N in the Atlantic, *Science*, *317*, 938–941, doi:10.1126/science.1141293.

Kanzow, T., H. L. Johnson, D. P. Marshall, S. A. Cunningham, J. J.-M. Hirschi, A. Mujahid, and H. L. Bryden (2009), Basinwide integrated volume transports in an eddy-filled ocean, *J. Phys. Oceanogr.*, *39*, 3901–3110, doi:10.1175/2009JPO4185.1.

Kanzow, T., et al. (2010), Seasonal variability of the Atlantic meridional overturning circulation at 26.5°N, *J. Clim.*, *23*, 5678–5698, doi:10.1175/2010JCLI3389.1

Losch, M., D. Menemenlis, J. M. Campin, P. Heimbach, and C. Hill (2010), On the formulation of sea-ice models. Part 1: Effects of different solver implementations and parameterizations, *Ocean Modell.*, *33*, 129–144, doi:10.1016/j.ocemod.2009.12.008.

Menemenlis, D., J. Campin, P. Heimbach, C. Hill, T. Lee, A. Nguyen, M. Schodlock, and H. Zhang (2008), ECCO2: High resolution global ocean and sea ice data synthesis, *Mercator Ocean Q. Newsl.*, *31*, 13–21.

Tierney, C., J. Wahr, F. Bryan, and V. Zlotnicki (2000), Short-period oceanic circulation: Implications for satellite altimetry, *Geophys. Res. Lett.*, *27*, 1255–1258.

Vinogradova, N. T., R. M. Ponte, and D. Stammer (2007), Relation between sea level and bottom pressure and the vertical dependence of oceanic variability, *Geophys. Res. Lett.*, *34*, L03608, doi:10.1029/2006GL028588.

S. Danilov, M. Losch, J. Schröter, and D. Sidorenko, Alfred Wegener Institute for Polar and Marine Research, Postfach 120161, D-27515 Bremerhaven, Germany.

V. O. Ivchenko, National Oceanography Centre, European Way, Southampton SO14 3ZH, UK. (voi@noc.soton.ac.uk)